Carbohydrate Polymers 266 (2021) 118153

Contents lists available at ScienceDirect

Carbohydrate Polymers

journal homepage: www.elsevier.com/locate/carbpol

Structural changes of bacterial cellulose due to incubation in conditions simulating human plasma in the presence of selected pathogens

Paulina Dederko-Kantowicz [a,b], Agata Sommer [a], Hanna Staroszczyk [a,*]

[a] Department of Chemistry, Technology and Biotechnology of Food, Chemical Faculty, Gdańsk University of Technology, Narutowicza 11/12 St. 80-233 Gdańsk, Poland
[b] Laboratory of Molecular Diagnostics and Biochemistry, Plant Breeding and Acclimatization Institute - National Research Institute, Bonin Research Center, Bonin 3, 76-009 Bonin, Poland

ARTICLE INFO

Keywords:
Bacterial nanocellulose
In vitro biodegradation
Structural characteristics

ABSTRACT

Bacterial nanocellulose (BNC) is a natural biomaterial with a wide range of medical applications. However, it cannot be used as a biological implant of the circulatory system without checking whether it is biodegradable under human plasma conditions. This work aimed to investigate the BNC biodegradation by selected pathogens under conditions simulating human plasma. The BNC was incubated in simulated biological fluids with or without *Staphylococcus aureus*, *Candida albicans* and *Aspergillus fumigatus,* and its physicochemical properties were studied. The results showed that the incubation of BNC in simulated body fluid with *A. fumigatus* contributes more to its degradation than that under other conditions tested. The rearrangement of the hydrogen-bond network in this case resulted in a more compact structure, with an increased crystallinity index, reduced thermal stability and looser cross-linking. Therefore, although BNC shows great potential as a cardiovascular implant material, before use for this purpose its biodegradability should be limited.

1. Introduction

Bacterial nanocellulose (BNC) is a polysaccharide produced by Gram-negative bacteria species: *Gluconacetobacter* or *Acetobacter, Achromobacter, Aerobacter, Agrobacterium, Azotobacter, Pseudomonas, Rhizobium,* and Gram-positive bacteria species such as *Sarcina ventriculi* (Wang et al., 2019). It was demonstrated that the most productive BNC-producers come from genera *Acetobacter* and *Komagataeibacter* (He et al., 2020). Due to unique properties including high chemical purity (no lignin and hemicelluloses), high mechanical strength and the ability to form any shape and size, BNC can be an alternative to the current materials used for cardiac-related applications, such as synthetic protheses made of polypropylene and biological protheses made of animal materials. Compared to the cost of obtaining synthetic polymers materials, BNC membrane preparation is relatively inexpensive, and unlike the biological tissues, BNC membranes are readily available. Moreover, synthetic and biological protheses are not always well tolerated by host tissues, while BNC meets biomaterials requirements: it is non-mutagenic, non-toxic and non-teratogenic (Wang et al., 2019). Also, it shows good blood compatibility when tested in vitro and in vivo (Malm et al., 2012). However, a question arises about the degradation of BNC-based material, as current research data shows that all polymer materials under human conditions are susceptible to biodegradation (Franceschini, 2019; Kidane et al., 2009). Cellulosic materials can be degraded by the action of various microorganisms. Most of them belong to eubacteria and fungi, although some anaerobic protozoa and slime molds capable of degrading cellulose have also been described (Pérez et al., 2002).

A biological implant is generally not exposed to microbiological infections for a long time after implantation because it is surrounded by tissue immediately after implantation. The highest risk of infection is associated with surgical procedure, i.e. with a surgical site infection (SSI) (Meakins, 2008). SSI is a type of nosocomial infection that can develop within a one-year surgery if artificial materials are used. It is estimated that such infections constitute 2–7% of all surgical procedures (Meakins, 2008). These can affect not only the skin or muscles at the

Abbreviations: A. fumigatus, Aspergillus fumigatus; BNC, bacterial nanocellulose; *C. albicans*, *Candida albicans*; CrI, crystallinity index; DTG, differential thermogravimetric curve; FT-IR, Fourier transformation infrared spectroscopy; HBI, hydrogen bond intensity; LOI, lateral order index; PBS, phosphate buffered saline; *S. aureus*, *Staphylococcus aureus*; SBF, simulated body fluid; SEM, scanning electron microscopy; SSI, surgical site infection; TCI, total crystallinity index; TG, thermogravimetric curve; TGA, thermogravimetric analysis; XRD, X-ray Diffractometry.

* Corresponding author.
E-mail addresses: p.dederko@ihar.edu.pl (P. Dederko-Kantowicz), agata.sommer@pg.edu.pl (A. Sommer), hanna.staroszczyk@pg.edu.pl (H. Staroszczyk).

https://doi.org/10.1016/j.carbpol.2021.118153
Received 22 December 2020; Received in revised form 25 April 2021; Accepted 30 April 2021
Available online 5 May 2021

incision site (Siondalski, Keita, et al., 2005; Siondalski, Roszak, et al., 2005) but, unfortunately, the operated organ too (Meakins, 2008). In the case of cardiovascular surgery procedures, SSI is the most severe complication with an incidence of up to 30% (5% of which are mediastinitis) (Borowiec, 2010; Gualis et al., 2009; Le Guillou et al., 2011). Additional risk factors for the occurrence of SSIs in cardiac surgery patients are comorbidities causing difficult wound healing, such as diabetes, respiratory or circulatory failure (Cheadle, 2006), and the use of immunosuppressants peri-implantation period. Other infections that can spread to tissue at the surgery site may be further risk factor (Kowalik et al., 2018; Le Guillou et al., 2011). Endocarditis is one such complication (Siondalski et al., 2003; Siondalski, Keita, et al., 2005). In turn, PCR tests allowed to detect temporary bacteraemia among the patients after the cardiosurgical operations connected with extracorporeal blood circulation (Siondalski et al., 2004). While coagulase-negative staphylococci are predominant in all of these infections, *Staphylococcus aureus*, *Candida albicans,* and *Aspergillus* are also prevalent with superinfection. Bacteria that most often infect the surgical wound itself in cardiac surgery procedures are *S. aureus,* often those constituting the physiological bacterial flora of the skin, which during the procedure are transferred to deeper tissues (Borowiec, 2010). Due to such a high risk of microbiological infections in cardiosurgical procedures, it is essential to check the influence of these microorganisms on the implant itself, whether these microorganisms will not cause its structure degradation, thus not disturbing its proper functioning after implantation.

The study aimed to determine the in vitro biodegradability of BNC in an environment simulating blood plasma in terms of its use as a material for cardiac implants production. As the in vivo biodegradation process can accelerate the growth of pathogenic microorganisms, their effect on biodegradation was also studied. The BNC before and after its incubation in simulated biological fluids in the presence or absence of *S. aureus*, *C. albicans* and *A. fumigatus* was characterized based on its morphology, crystallinity, and its chemical structure. The effect of incubation on the BC thermal stability was also evaluated. The presented results can answer the question whether the native BNC can be recommended for use as a non-biodegradable material in cardiovascular implants.

2. Experimental procedure

2.1. Materials

Bacterial nanocellulose (BNC), obtained according to the method described in patents: PL 171952 B1(Gałas & Krystynowicz, 1993), PL 212003 B1 (Krystynowicz et al., 2003) and US 6429002 (Ben-Bassad et al., 2002) was supplied by Bowil Biotech Ltd. (Władysławowo, Poland). A phosphate buffered saline (PBS, No. 524650) was purchased from Merck Ltd. Bacteria *S. aureus* PCM 2054 came from the Polish Collection of Microorganisms in the Institute of Immunology and Experimental Therapy (Polish Academy of Sciences in Wroclaw). Yeast *C. albicans* ATCC 10231 and mould *A. fumigatus* var. *fumigatus* ATCC 96918 were purchased from the American Type Culture Collection.

2.2. Methods

2.2.1. Preparation of phosphate buffered saline and a simulated body fluid

A PBS was prepared in accordance with the producer's instructions and sterilized in an autoclave at 115 °C for 20 min. A simulated body fluid (SBF) was prepared by dissolving the mineral components in distilled water, according to Chavan et al. (2010). The resulting solution was adjusted to pH 7.4 with 6 M HCl and then filtered through the filters with a 45 μm pore size using a Millipore vacuum filtration kit. To obtain a sterile SBF fluid, it was subjected to tyndallization after filtration, i.e. three times pasteurization at 100 °C for 30 min, at 24-hour intervals. No microbial growth during storage at 37 °C for 6 months was observed in the SBF prepared in this way.

2.2.2. Culture and growth conditions of microorganisms

Cultures of microorganisms by inoculating 100 mL of Tryptic Soy Broth, pH 7.0 (*S. aureus)*, or 100 mL of Maltose Soy Broth, pH 5.6 (*C. albicans* and *A. fumigatus*) with 0.1 mL of liquid culture (at stationary phase of growth) and incubating it with shaking at 37 °C for 24 h (bacteria and yeast) or 72 h (mould) were prepared.

2.2.3. Susceptibility to biodegradation assay of BNC

The susceptibility of BNC to biodegradation in the absence and in the presence of microorganisms was carried out. In the first case, never dried samples of sterile BNC membrane cut into square shape (25 × 25 mm) were stored for six months at 37 °C in 150 mL of sterile PBS and 62.5 mL of sterile SBF. In the second case, cultures of *S. aureus*, *C. albicans* and *A. fumigatus*, in the stationary phase of growth, were added to SBF, with or without BNC, to a final concentration of about 10^3 CFU/mL (CFU – colony-forming unit). Such a high concentration of the microorganisms was applied to accelerate their effect on the material under study. All samples were incubated for six months at 37 °C with at least four of each sample tested.

Changes in the BNC samples' structural and thermal properties and surface morphology were determined at selected time intervals. All samples were freeze-dried and conditioned before analysis for seven days in a P_2O_5.

2.2.4. Scanning electron microscopy (SEM)

Surface morphology changes in incubated BNC samples was examined by means of a Dual Beam Versa 3D (FEI Company, Eidhoven, The Netherlands) instrument equipped with a *field emission gun* (FEG). The instrument, set for 5 kV accelerating voltage and 1,6 pA or 3,3 pA beam current. The instrument was operated at high vacuum. The magnification range changed from 15,000 to 25,000 times.

2.2.5. X-ray diffractometry (XRD)

The measurements using Cu Kα radiation of wavelength 0.154 nm on a Phillips type X'pert diffractometer were carried out. The operation setting for the diffractometer was 30 mA and 40 kV. The spectra over the range of 4.0–40.0° 2θ were recorded at a scan rate of 0.02° 2 θ /s.

The crystallinity index (CrI) of BNC samples was calculated based on the equation proposed by Segal et al. (1959).

$$CrI = \frac{(I_{200} - I_{am})}{I_{200}} \times 100$$

where I_{200} and I_{am} are the maximum intensities of diffraction at 2θ = 22,7 and 18°, respectively.

2.2.6. Thermogravimetric analysis (TGA)

The analyses on 10–20 mg samples were performed. They were heated in the open corundum crucibles in a nitrogen atmosphere over a temperature range of 30–700 °C. The 10 °C/min rate of the temperature increase was applied. The instrument of SDT Q600 (TA Instruments-Water LLC, New Castle, DE) was used.

2.2.7. Fourier transformation infrared spectroscopy (FT-IR)

FT-IR spectra of BNC samples were recorded in the range of 4000–500 cm^{-1} with 32 scans at a resolution of 4 cm^{-1}. A Nicolet 8700 spectrometer (Thermo Electron Scientific Inc) equipped with a diamond crystal Golden Gate (Specac) ATR accessory to collect spectra was used. The reflectance element was a diamond crystal. To assess precision and ensure the reproducibility of each sample, three to five replicate spectra for each sample aliquot were recorded.

The second derivatives of the spectra were calculated by using the Savitzky-Golay algorithm (27 data points, ca. 25 cm^{-1}, and a 3rd degree polynomial) in order to resolve the overlapping bands of individual vibrations in the region 3600–3000 cm^{-1}.

To study the crystallinity changes, total crystallinity index (TCI)

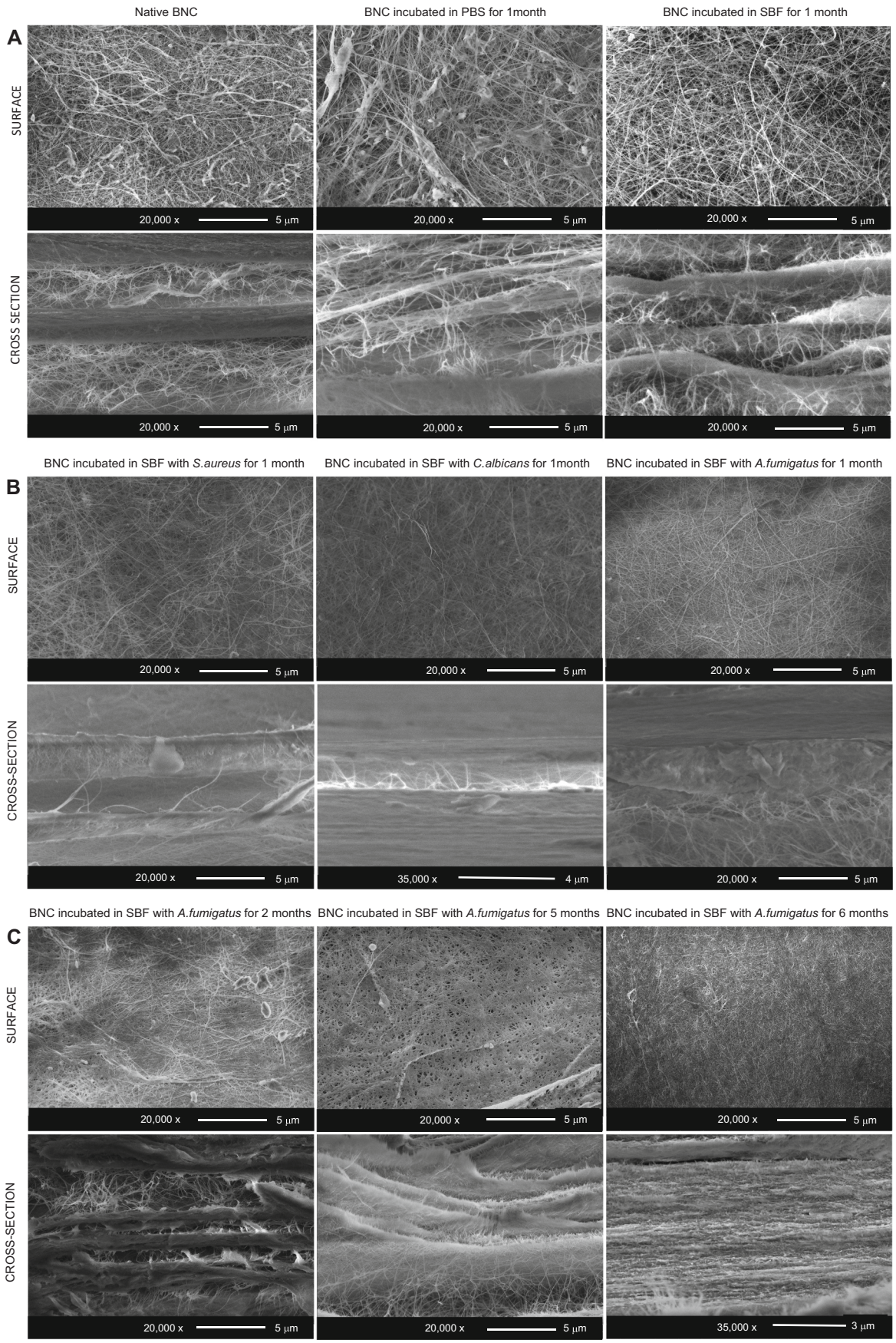

Fig. 1. The scanning electron micrographs of the surface and the cross-section of the native BNC and the BNC incubated in the sterile PBF and SBF for one month (A), in the SBF with all microorganisms tested for one month (B), and in the SBF with *A. fumigatus* for 2, 5 and 6 months.

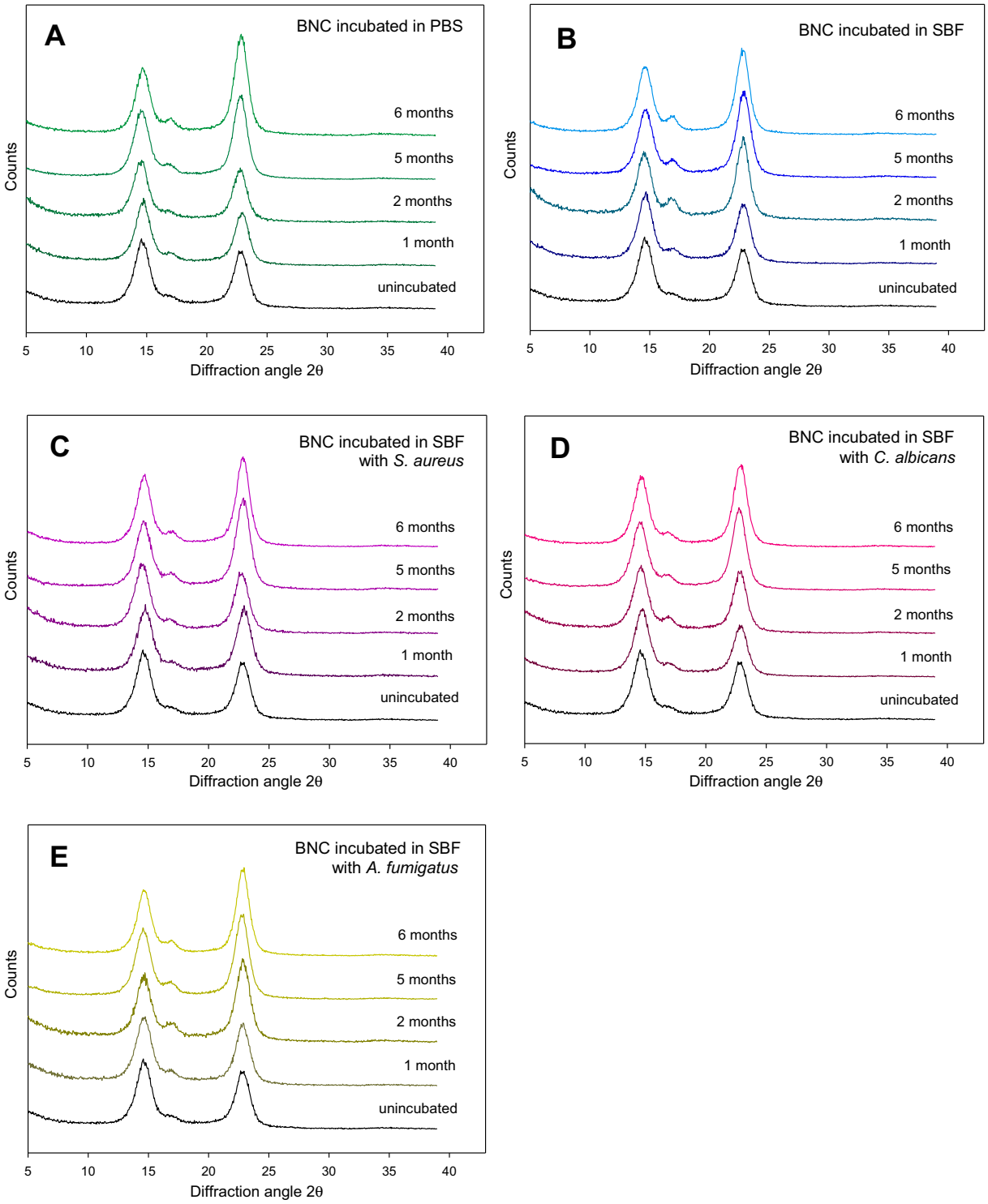

Fig. 2. XRD diffractograms of the native BNC (unincubated) and the BNC incubated for selected time intervals in the sterile PBS (A) and SBF (B), and in the SBF with *S. aureus* (C), *C. albicans* (D), and *A. fumigatus* (E).

(Nelson & O'Connor, 1964), lateral order index (LOI) (Hurtubise & Krassig, 1960; Nelson & O'Connor, 1964), and hydrogen bond intensity (HBI) (Nada et al., 2000), calculated from the absorbance ratios $A_{1372}/A_{2897\ (2892?)}$, $A_{1430\ (1429?)}/A_{893}$, and A_{3336}/A_{1336}, respectively, were used.

2.3. Statistical analysis

All data obtained were statistically analyzed by one-way analysis of variance to determine significant differences among BNC samples, using SigmaPlot 11.0 (Softonic International 170 S.L.). Significance at $p < 0.05$ was accepted.

Table 1
Changes in the crystallinity index (CrI)[a] of the BNC incubated over one to six months.

BNC incubated	sterile PBS	sterile SBF	SBF with *S. aureus*	SBF with *C. albicans*	SBF with *A. fumigatus*
1 month	95.4	94.8	94.3	94.3	95.0
2 months	97.0	98.1	97.4	97.5	96.3
5 months	95.5	97.4	96.6	96.3	96.6
6 months	94.7	96.3	94.8	95.2	97.4

[a] CrI of the native BNC was 94.7%.

3. Results and discussion

3.1. BNC characterization by analysis of SEM images

The SEM revealed a homogeneous structure on the surface of native BNC with a clearly visible, single fibers and with irregularly spaced pores (Fig. 1A). In the SEM image of the cross-section of native BNC, 3D, well-organized structure with parallel arranged layers was observed. Such a bacterial cellulose structure has already been reported and described before (Moon et al., 2011 and references therein). According to Gama et al. (2017), cellulose fibers interact with each other and are kept separate by adsorbed water layers due to hydrogen bonding and van der Waals forces.

BNC's surface morphology did not change significantly after its membranes were incubated in sterile PBS and SBF for both one month (Fig. 1A) and six months (images not presented), only a slight relaxation of the structure was observed. After a month incubation of membranes in SBF in the presence of *S. aureus*, *C. albicans* and *A. fumigatus,* the surface became less homogeneous (Fig. 1B) compared to that of the non-incubated sample (Fig. 1A), with fewer individual fibers visible between the cellulose layers in the cross-section. Prolonged incubation led to a reduction of the distances between these fibers, which, in turn, led to the more compact structure, the most pronounced in the case of BNC incubated in the SBF with *of A. fumigatus*, (1C). It can be assumed that the observed changes, especially in the latter case, were due to degradation of the BNC by the microorganisms tested.

3.2. BNC characterization by analysis of XRD diffractograms

The physicochemical analysis confirmed that there were changes in BNC structure due to the incubation of its membranes under conditions simulating human plasma. While the XRD diffractogram of native BNC was characterized by two sharp, intense peaks at 14,6° and 22,7° 2θ angle, the diffractograms of BNC incubated under all studied conditions showed a decrease in the intensity of the former, and an increase in the latter peak as the incubation time increased (Fig. 2). As with the morphological changes observed in the SEM images, also these changes were the most visible in the diffractograms of BNC incubated in SBF with *A. fumigatus.* Since the peaks located at 14.6° and 22.6° 2θ are assigned to I_α and I_β crystalline form, respectively, in which polysaccharide chains are similar in parallel configurations, but for differences in the arrangement of the hydrogen-bond network (Oh et al., 2005), the changes observed indicate that the rearrangement of the hydrogen-bond network in the BC structure occurred.

The crystallinity index (CrI) of native BNC amounted to 94.7% (Table 1). Upon the month incubation of the membranes in sterile PBS and SBF, and in SBF with *S. aureus* and *C. albicans*, the CrI remained virtually unchanged. After the two-months incubation, it was increased, and after the five- and six-months incubation it was gradually decreased; however, to the value not less than that of the CrI of native BNC. In the BNC incubated in SBF with *A. fumigatus*, the gradually increase of the CrI was observed, from 95% for the BNC incubated for one month to 97.4% for the BNC incubated for six months. Shi et al. (2014) demonstrated a reduction of crystallinity degree of BNC incubated in PBS buffer for two

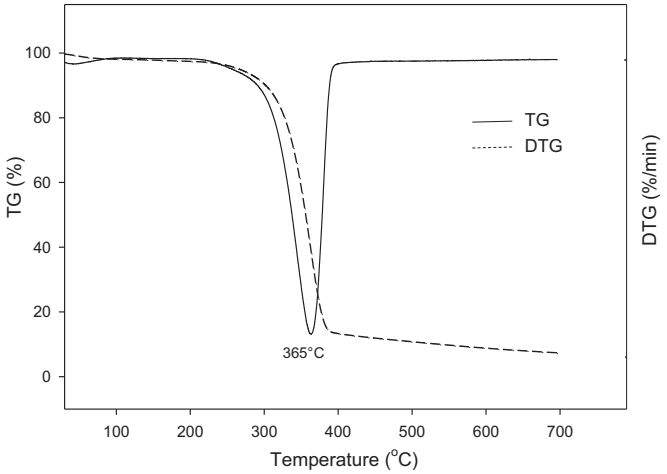

Fig. 3. Thermogram of native BNC.

Table 2
Thermogravimetric characteristics of the native BNC.

Temperature range (°C)	Weight loss (%)[a]	DTG (°C)
35–200	4	
200–400	85	365
400–700	11	

[a] Percentage of weight loss during the special temperature ranges.

months. According to the authors, the crystallinity degree is reduced by ca. 30% due to the swelling of the polymer under these conditions and a penetration of water into its crystalline regions, which lead to a change in the arrangement of the polysaccharide chains and an expansion of amorphous regions. In turn, Wang et al. (2016) observed ca. 70% decrease in the crystallinity degree of the BNC incubated for eight weeks in the presence of cellulases. According to these authors, the cellulases cause the fragmentation of polysaccharide chains. BNC crystalline regions gradually turn into amorphous ones, leading to a reduction in the crystallinity degree. The cellulases used by the authors were commercial enzyme preparations, being a mixture of *endo-* and exoglucanase and β-glucosidase. Ljungdahl and Eriksson (1985) proved that endo-β-1,4-glucanases randomly cleave β-(1 → 4)-glycosidic bonds along the cellulose chain, *exo*-β-1,4-glucanases cleave cellobiosis or glucose from the non-reducing end of cellulose, and β-1,4-glucosidases hydrolyze cellobiosis to two glucose molecules. According to the authors, amorphous cellulose regions can be degraded by both endo- and exoglucanases, while degradation of crystal regions requires synergic action of both types of enzymes. It seems therefore that the microorganisms used in the presented studies, *S. aureus*, *C. albicans* and *A. fumigatus*, were not able to produce all enzymes necessary to degrade cellulose to the same extent, and therefore the CrI of BNC incubated in the presence of each of them was different. According to Chandra and Rustgi (1998), *A. fumigatus* can produce cellulose hydrolyzing enzymes, while bacteria and yeasts can periodically make endo- and exoenzymes only when they have no access to other carbon sources. The gradually increasing crystallinity degree of the BNC after the incubation its membranes in the SBF with *A. fumigatus* over one to six months (Table 1) could be the result of the action of cellulolytic enzymes produced by them capable of degrading the amorphous regions of the BNC. It made the BNC more crystalline and therefore its further degradation was difficult. These findings confirm the previous reports (Norkrans, 1950; Walseth, 1957).

3.3. BNC characterization by analysis of TGA thermograms

Thermogram of native BNC (Fig. 3) revealed the one step

Table 3
Thermogravimetric characteristics of BNC incubated in the sterile PBS and SBF, and SBF with *S. aureus, C. albicans and A. fumigatus*.

BNC incubated	Temperature range (°C)	PBS		SBF		SBF with *S. aureus*		SBF with *C. albicans*		SBF with *A. fumigatus*	
		Weight loss (%)[a]	DTG (°C)	Weight loss (%)[a]	DTG (°C)	Weight loss (%)[a]	DTG (°C)	Weight loss (%)[a]	DTG (°C)	Weight loss (%)[a]	DTG (°C)
1 month	35–200	3		3		2		3		4	
	200–400	88	366	85	365	87	364	89	366	85	356
	400–700	7		12		10		8		11	
	Total	98		100		99		100		100	
2 months	35–200	4		4		4		3		4	
	200–400	95	372	91	366	92	370	93	369	90	359
	400–700	1		5		4		4		5	
	Total	100		100		100		100		99	
5 months	35–200	2		2		2		2		2	
	200–400	85	365	89	373	85	366	87	368	83	354
	400–700	13		9		13		11		15	
	Total	100		100		100		100		100	
6 months	35–200	5		6		6	169	6	166	7	167
	200–400	82	364	82	366	84	365	83	367	78	355
	400–700	13		12		10		11		15	
	Total	100		100		100		100		100	

[a] Percentage of weight loss during the special temperature ranges.

Table 4
Band assignment in the FT-IR spectra of native BNC.

Band position (cm^{-1}) and intensity[a]	Band assignment	References
3405 sh	ν_{OH} intramolecular H-bonds for 3O···H–O5 and 2O···H–O6	Carrilo et al., 2004; Goswami & Das, 2019; Sugiyama et al., 1991
3344 vs	ν_{OH} intramolecular H-bonds for 3O···H–O5	Abidi et al., 2010; Carrilo et al., 2004; Halib et al., 2012; Misra et al., 2020
3310 sh	ν_{OH} intermolecular H-bonds	Sugiyama et al., 1991
3244 m	ν_{OH} intermolecular H-bonds for 6O···H–O3'	Abidi et al., 2010
2897 m	ν_{CH}, ν_{CH2}	Abidi et al., 2010; Goh et al., 2012; Goswami & Das, 2019; Oh et al., 2005; Halib et al., 2012; Shi et al., 2014
1635 w	δ_{OH} polymer bound water	Abidi et al., 2010; Goswami & Das, 2019; Misra et al., 2020
1427 m	δ_{OH}, δ_{CH}	Oh et al., 2005; Misra et al., 2020
1369 w	δ_{OH}, δ_{CH}	Carrilo et al., 2004; Goh et al., 2012; Hishikawa et al., 2017; Misra et al., 2020
1336 w	δ_{OH}	Oh et al., 2005
1315 m	δ_{CH2}	Halib et al., 2012; Kacuráková et al., 2002
1281 w	δ_{CH}	Carrilo et al., 2004
1161 m	δ_{C-O-C} of C1–O–C4	Abidi et al., 2010; Oh et al., 2005; Halib et al., 2012
1107 s	δ_{C-OH} of C2–OH	Kacuráková et al., 2002
1055 vs	δ_{C-OH} of C3–OH	Halib et al., 2012; Kacuráková et al., 2002
1032 vs	δ_{C-OH} of C6–OH	Halib et al., 2012; Kacuráková et al., 2002
1003 vs	ν_{C-O}	Kacuráková et al., 2002
985 s	ν_{C-O}	Abidi et al., 2010
899 m	β-glycosidic linkage	Kacuráková et al., 2002; Misra et al., 2020
750 w	I_{α}, δ_{OH} out-of-plane	Liu et al., 2010; Sugiyama et al., 1991
710 w	I_{β}, δ_{OH} out-of-plane	Abidi et al., 2010; Liu et al., 2010; Sugiyama et al., 1991

[a] vs – very strong; s – strong; m – medium; w – weak; sh - shoulder.

decomposition of that cellulose at 365 °C with the weight loss of 85% within the range of 200–400 °C (Table 2). Saska et al. (2011) and Halib et al. (2012) showed a lower decomposition temperature of native BNC, which was 333, 342 and 352 °C, respectively. The difference in the decomposition temperature of BNC could result from the different strains used to the culture of BNC and the other culturing conditions. Unfortunately, the authors did not provide either names of used bacterial strains nor their culture conditions.

The thermogram patterns of all samples tested remained essentially the same as that of native BNC, but they showed different decomposition temperatures (Table 3).

Upon the one-month incubation in the sterile PBS and SBF, and in the SBF with *S. aureus* and *C. albicans*, the decomposition temperature of BNC maintained at the level of that of native BNC, after the two-months incubation it was increased several degrees, and after the five- and six-months incubation it was gradually decreased to the temperature characteristic of native BNC. On the other hand, the degradation temperature of BNC incubated in the SBF with *A. fumigatus* was reduced by ca. 10 °C already after the first month and remained at that level for the next months of incubation. Such changes in the thermal properties of the BNC incubated in the SBF with *A. fumigatus* reflect a decrease in its degree of cross-linking with hydrogen bonds. As a result of the action of cellulolytic enzymes produced by these microorganisms, the BNC become less cross-linked and thus less thermally stable.

All BNC samples incubated for six months in the SBF with microorganisms showed an additional decomposition step at temperature ca.167 °C, losing ca. 6% more of their weight within the 35–200 °C range than the native BNC and the BNC incubated for a shorter time. The higher water content in the BNC after the six-months of incubation was probably the result of its progressive degradation. As shown in our previous studies, the BNC membranes, after such time of incubation in the SBF with microorganisms, were swelled, and their wet mass was increased (Dederko et al., 2018). Shi et al. (2014) noted a swelling of BNC membranes immersed in a PBS buffer. According to the authors, the strength of hydrogen bonds between OH groups of polymer chains decreases after its immersion, which leads to their breaking. The breaking of the hydrogen bonds between the chains, in turn, allows the formation of new hydrogen bonds between the OH groups polysaccharide and water molecules.

3.4. BNC characterization by analysis of FTIR spectra

Table 4 lists the band assignment in the FT-IR spectrum of native BNC. As Halib et al. (2012) reported, the strain used to the culture of BNC and the measurement conditions can result in subtle changes in the position and the intensity of the bands in the FTIR spectra of bacterial cellulose.

No significant differences in the FTIR spectrum of BNC after its

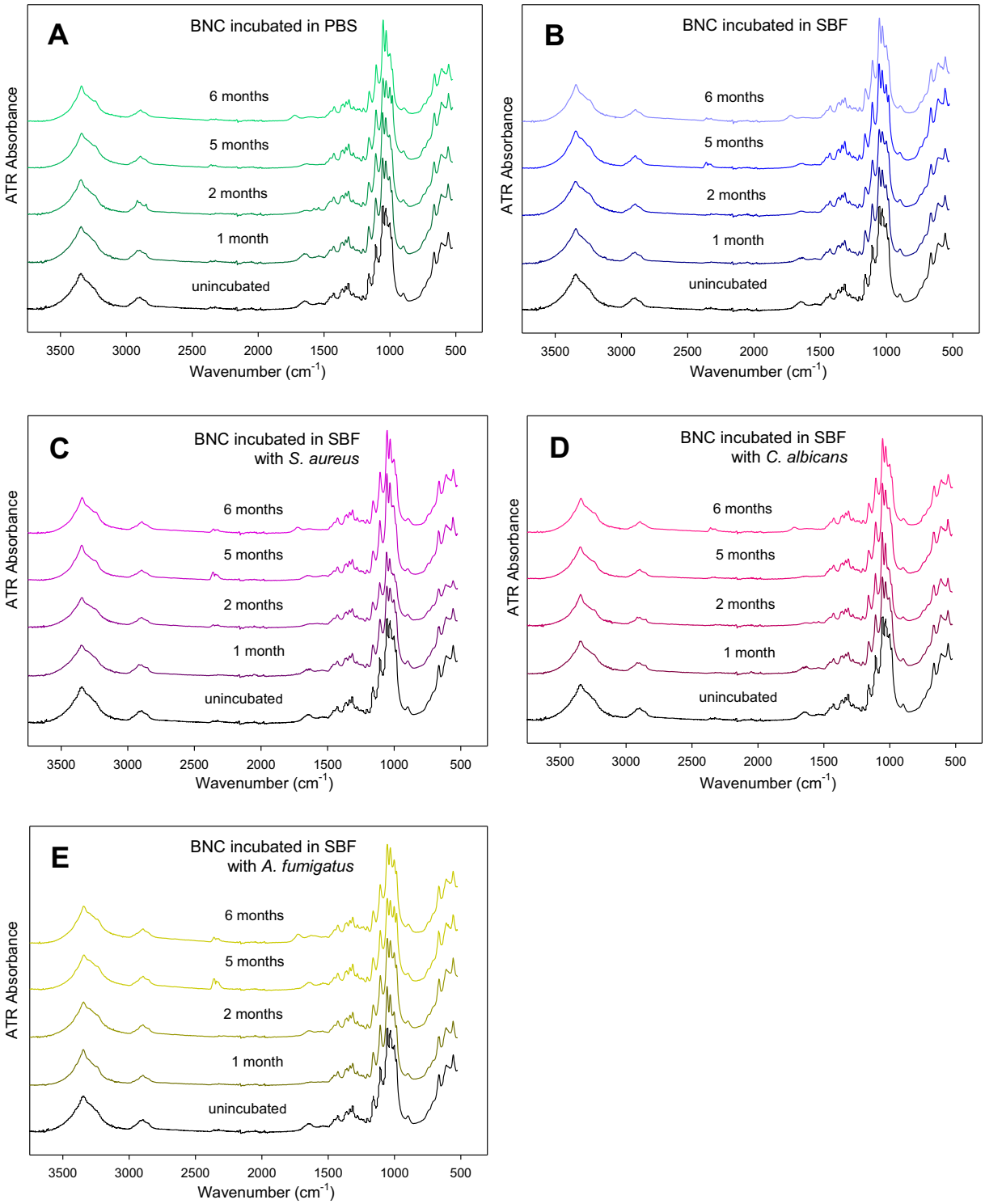

Fig. 4. FT-IR spectra of the native BNC (unincubated) and the BNC incubated for selected time intervals in the sterile PBS (A) and SBF (B), and in the SBF with *S. aureus* (C), *C. albicans* (D), and *A. fumigatus* (E).

incubation for one-six months in the sterile PBS and SBF, and in SBF in the presence of microorganisms tested were observed (Fig. 4). However, the band intensity with the maximum at 1635 cm^{-1} gradually decreased as the incubation period increased, showing the water content changes in the samples tested (Table 4).

Moreover, the second-derivative procedure used, which allows more specific identification of the band at the 3600–3000 cm^{-1} region, enabled to resolve of this band into its four components, located at 3410, 3349, 3296, and 3235 cm^{-1} in the spectrum of the native BNC (Fig. 5). While in the spectra of the BNC incubated in sterile PBS and SBF, and in the BNC incubated in SBF with *S. aureus* and *C. albicans,* the maxima of these bands remained at the same wavenumbers or shifted only slightly, in the spectra of the BNC incubated in SBF with *A. fumigatus* clear shifts by 3–9 cm^{-1} towards lower wavenumbers were observed. As the former pair of peaks is assigned to intra-, and the latter to intermolecular hydrogen bonds (Hishikawa et al., 2017; Oh et al., 2005), the observed

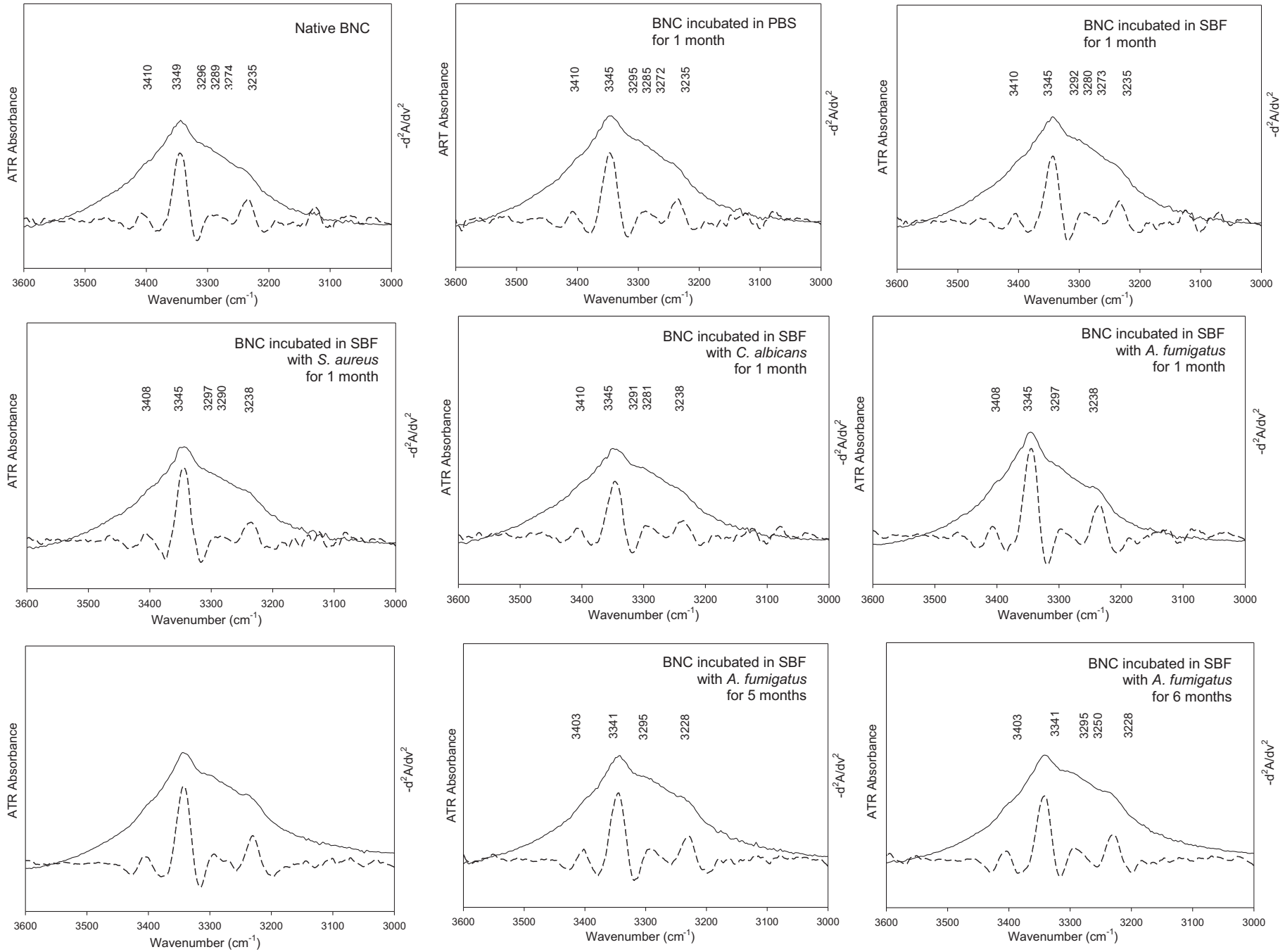

Fig. 5. Absorbance (—) and second-derivative (———) spectra of the native BNC and the BNC incubated for selected time intervals in the sterile PBS and SBF, and in the SBF with microorganisms tested.

Table 5
Effect of the incubation on the HBI, TCI, and LOI indexes of BNC[a], mean value of 3 measurements (standard deviation was below 0.1 in each case).

BNC incubated	Sterile PBS			Sterile SBF			SBF with *S. aureus*			SBF with *C. albicans*			SBF with *A. fumigatus*		
	HBI	TCI	LOI	HBI	TCI	LOI	HBI	TCI	LOI	HBI	TCI	LOI	HBI	TCI	LOI
1 month	1.9	1.1	0.8	1.9	1.0	1.0	1.7	1.0	1.2	2.0	1.1	1.8	2.0	1.0	1.6
2 months	2.0	1.1	1.2	2.0	0.8	1.7	2.1	1.2	1.9	2.3	1.1	1.9	1.6	1.0	1.5
5 months	1.9	1.2	1.8	2.1	1.0	2.0	1.9	1.2	2.3	2.3	1.0	1.8	1.6	1.1	1.8
6 months	1.9	1.0	1.7	1.9	1.0	1.4	1.7	1.1	2.5	2.0	1.0	1.5	1.5	1.1	1.8

[a] HBI, TCI LOI of the native BNC was 1.9, 0.9, and 1.0, respectively.

changes seem to confirm the results of the thermal analysis, and it indicate the scission of these bonds in the BNC due to the incubation of its membranes in these conditions. Since loose cross-linked membranes are less resistant to media penetration in the network than those of densely cross-linked, their degradation is increasing. Additionally, the 3600–3000 cm^{-1} band has been described as indicative of water-mediated hydrogen bonding (Yakimets et al., 2007). The breaking of these bonds probably released water molecules and hence in thermograms of the BNC incubated for six months the higher water content was noted.

In order to estimate qualitative changes in the crystallinity of cellulose, HBI, LOI and TCI indexes were calculated. An insight in the Table 5 confirmed that the number of hydrogen bonds (HBI index) in the BNC decreased with increasing time of the incubation of its membrane in the SBF with *A. fumigatus*, while LOI and TCI indexes increased. This means that due to the incubation of BNC in these conditions its crystallinity increased. The observed trend is in line with previous findings (Kljun et al., 2011) and designed indexes were strongly correlated with those observed from XRD and TGA measurements.

4. Conclusions

The in-vitro biodegradability of BNC under conditions simulating human plasma both in the presence and absence of *S. aureus, C. albicans* and *A. fumigatus* was checked. The incubation under conditions tested, especially in SBF with of *A. fumigatus*, led to the more compact structure, what was the result of the rearrangement of the hydrogen-bond network in the BC structure. The increasing crystallinity degree of the BNC after the incubation in SBF with *A. fumigatus* resulted from the action of cellulolytic enzymes produced by them capable of degrading the amorphous regions of the BNC. As a result of the action of these enzymes, BNC has become less cross-linked and therefore less thermally stable. Since loose cross-linked membranes are less resistant to media penetration in the network than those of densely cross-linked, their degradation was increasing.

The presented studies, together with previous experimental data (Kołaczkowska et al., 2019; Stanisławska et al., 2020), indicate the potential of BNC for the production of cardiovascular implants. However, it has been shown that its biodegradability should be reduced. Further research is therefore necessary.

CRediT authorship contribution statement

Paulina Dederko-Kantowicz: Formal analysis, Investigation, Data curation, Writing - original draft, Visualization. Agata Sommer: Formal analysis, Data curation, Visualization. Hanna Staroszczyk: Conceptualization, Supervision, Project administration, Funding acquisition, Writing - review and editing.

Acknowledgments

This work was supported by the Polish national research budget, under the National Centre Research and Development grant number PBS2/A7/16/2013 entitled "Research on the use of bacterial nanocellulose (BNC) in regenerative medicine as a function of the biological implants in cardiac and vascular surgery". The research was conducted in an interdisciplinary group of experts from Gdańsk University of Technology (Gdańsk, Poland), Medical University of Gdańsk (Gdańsk, Poland), University of Gdańsk (Gdańsk, Poland), Zbigniew Religa Fundation of Cardiac Surgery Development (Zabrze, Poland), Maritime Advanced Research Centre S. A. (Gdańsk, Poland), Bowil Biotech Ltd. (Władysławowo, Poland).

The authors would like to thank Edyta Malinowska-Pańczyk from the Gdańsk University of Technology for her help in planning all microbiological tests and dedicate this paper to the memory of Ilona Kołodziejska, who passed away in 2016, and worked as a co-investigator in the project.

References

Abidi, N., Cabrales, L., & Hequet, E. (2010). Fourier transform infrared spectroscopic approach to the study of the secondary cell wall development in cotton fiber. *Cellulose, 17*, 309–320. https://doi.org/10.1007/s10570-009-9366-1

Ben-Bassad, A., Burner, R., Shoemaker, S., Aloni, Y., Wong, H., Johnson, D. C., et al. (2002). Reticulated cellulose producing Acetobacter strains. US 6,426,002 B.

Borowiec, J. (2010). Surgical site infections in cardiac surgery – "Vision zero". *Medicine, Kardiochirurgia i Torakochirurgia Polska, 7*, 383–387 (in Polish).

Carrilo, F., Colom, X., Suñol, J. J., & Saurina, J. (2004). Structural FTIR analysis and thermal characterization of lyocell and viscose-type fibres. *European Polymer Journal, 40*, 2229–2234. https://doi.org/10.1016/j.eurpolymj.2004.05.003

Chandra, R., & Rustgi, R. (1998). Biodegradable polymers. *Progress in Polymer Science, 23*, 1273–1335. https://doi.org/10.1016/S0079-6700(97)00039-7

Chavan, P. N., Bahir, M. M., Mene, R. U., Mahabole, M. P., & Khairnar, R. S. (2010). Study of nanobiomaterial hydroxyapatite in simulated body fluid: Formation and growth of apatite. *Materials Science and Engineering B, 168*, 224–230.

Cheadle, W. G. (2006). Risk factors for surgical site infection. *Surgical Infections, 7*(s1), S7–11. https://doi.org/10.1089/sur.2006.7.s1-7

Dederko, P., Malinowska-Pańczyk, E., Staroszczyk, H., Sinkiewicz, I., Szweda, P., & Siondalski, P. (2018). *In vitro* biodegradation of bacterial nanocellulose under conditions simulating human plasma in the presence of selected pathogenic microorganisms. Polimery, 63, 372–380. doi:10.14314/polimery.2018.5.6.

Franceschini, G. (2019). Internal surgical use of biodegradable carbohydrate polymers. Warning for a conscious and proper use of oxidized regenerated cellulose. *Carbohydrate Polymers, 216*, 213–216. https://doi.org/10.1016/j.carbpol.2019.04.036

Gałas, E. & Krystynowicz, A. (1993). Sposób wytwarzania celulozy bakteryjnej. PL 171952 B1.

Gama, M., Gatenholm, P., & Klemm, D. (2017). *Bacterial nanocellulose: A sophisticated multifunctional material*. Boca Raton, London, New York: CRC Press.

Goh, W. N., Rosma, A., Kaur, B., Fazilah, A., Karim, A. A., & Bhat, R. (2012). Microstructure and physical properties of microbial cellulose produced during fermentation of black tea broth (Kombucha). *International Food Research Journal, 19*, 153–158.

Goswami, M., & Das, A. M. (2019). Synthesis and characterization of a biodegradable cellulose acetate-montmorillonite composite for effective adsorption of Eosin Y. *Carbohydrate Polymers, 206*, 863–872. https://doi.org/10.1016/j.carbpol.2018.11.040

Gualis, J., Flórez, S., Tamayo, E., Alvarez, F. J., Castrodeza, J., & Castaño, M. (2009). Risk factors for mediastinitis and endocarditis after cardiac surgery. *Asian Cardiovascular & Thoracic Annals, 17*, 612–616. https://doi.org/10.1177/0218492309349071

Halib, N., Amin, M. C. I. M., & Ahmad, I. (2012). Physcochemical properties and characterization of nata de coco from local food industries as a source of cellulose. *Sains Malaysiana, 41*, 205–211.

He, X., Meng, H., Song, H., Deng, S., He, T., Wang, S., Wei, D., & Zhang, Z. (2020). Novel bacterial cellulose membrane biosynthesized by a new and highly efficient producer *Komagataeibacter rhaeticus* TJPU03. *Carbohydrate Research, 493*, 108030. https://doi.org/10.1016/j.carres.2020.108030

Hishikawa, Y., Togawa, E., & Kondo, T. (2017). Characterization of individual hydrogen bonds in crystalline regenerated cellulose using resolved polarized FTIR spectra. *ACS Omega, 2*, 1469–1476. https://doi.org/10.1021/acsomega.6b00364

Hurtubise, F., & Krassig, H. (1960). Classification of fine structural characteristics in cellulose by infrared spectroscopy. *Analytical Chemistry, 32*, 177–181. https://doi.org/10.1021/ac60158a010

Kacuráková, M., Smith, A. C., Gidley, M. J., & Wilson, R. H. (2002). Molecular interactions in bacterial cellulose composites studied by 1D FT-IR and dynamic 2D FT-IR spectroscopy. *Carbohydrate Research, 337*, 1145–1153. https://doi.org/10.1016/S0008-6215(02)00102-7

Kidane, A. G., Burriesci, G., Cornejo, P., Dooley, A., Sarkar, S., Bonhoeffer, P., … Seifalian, A. M. (2009). Review. Current developments and future prospects for heart valve replacement therapy. *Journal of Biomedical Materials Research Part B: Applied Biomaterials, 88B*, 290–303. https://doi.org/10.1002/jbm.b.31151

Kljun, A., Benians, T. A. S., Goubet, F., Meulewaeter, F., Knox, J. P., & Blackburn, R. S. (2011). Comparative analysis of crystallinity changes in cellulose I polymers using ATR-FTIR, X-ray diffraction, and carbohydrate-binding module probes. *Biomacromolecules, 12*, 4121–4126. https://doi.org/10.1021/bm201176m

Kołaczkowska, M., Siondalski, P., Kowalik, M. M., Pęksa, R., Długa, A., Zając, W., et al. (2019). Assessment of the usefulness of bacterial cellulose produced by Gluconacetobacter xylinus E25 as a new biological implant. Materials Science & Engineering, C: Materials for Biological Applications, 97, 302–312. doi:10. 1016/j.msec.2018.12.016.

Kowalik, M. M., Lango, R., Siondalski, P., Chmara, M., Brzeziński, M., Lewandowski, K., Jagielak, D., Klapkowski, A., & Rogowski, A. (2018). Clinical, biochemical and genetic risk factors for 30-day and 5-year mortality in 518 adult patients subjected to cardiopulmonary bypass during cardiac surgery – The INFLACOR study. Acta Biochimica Polonica, 65, 241–250. doi:10.18388/abp.2017_2361.

Krystynowicz, A., Czaja, W., & Bielecki, S. (2003). Sposób otrzymywania celulozy bakteryjnej. PL 212003 B1.

Le Guillou, V., Tavolacci, M.-P., Baste, J.-M., Hubscher, C., Bedoit, E., Bessou, J.-P., & Litzler, P.-Y. (2011). Surgical site infection after central venous catheter-related infection in cardiac surgery. Analysis of a cohort of 7557 patients. *The Journal of Hospital Infection, 79*, 236–241. https://doi.org/10.1016/j.jhin.2011.07.004

Liu, Y., Gamble, G., & Thibodeaux, D. (2010). Development of Fourier transform infrared spectroscopy in direct, non-destructive, and rapid determination of cotton fiber maturity. *Applied Spectroscopy, 64*, 1355–1363. https://doi.org/10.1177/0040517511410107

Ljungdahl, L. G., & Eriksson, K. E. (1985). Ecology of microbial cellulose degradation. In K. C. Marshall (Ed.), *Advances in microbial ecology* (pp. 237–299). New York: Plenum Press.

Malm, C. J., Risberg, B., Bodin, A., Bäckdahl, H., Johansson, B. R., Gatenholm, P., & Jeppsson, A. (2012). Small calibre biosynthetic bacterial cellulose blood vessels: 13-months patency in a sheep model. *Scandinavian Cardiovascular Journal, 46*, 57–62. https://doi.org/10.3109/14017431.2011.623788

Meakins, J. (2008). Prevention of postoperative infection. Basic surgical and perioperative consideration. *ACS Surgery: Principles and Practice, 1*, 6–7.

Misra, N., Rawat, S., Goel, N. K., Shelkar, S. A., & Kumar, V. (2020). Radiation grafted cellulose fabric as reusable anionic adsorbent: A novel strategy for potential large-scale dye wastewater remediation. *Carbohydrate Polymers, 249*, 116902. https://doi.org/10.1016/j.carbpol.2020.116902

Moon, R. J., Martini, A., Nairn, J., Siomonsen, J., & Youngblood, J. (2011). Cellulose nanomaterials review: Structure, properties and nanocomposites. *Chemical Society Reviews, 40*, 3941–3994. https://doi.org/10.1039/C0CS00108B

Nada, A.-A. M. A., Kamel, S., & El-Sakhawy, M. (2000). Thermal behaviour and infrared spectroscopy of cellulose carbamates. *Polymer Degradation and Stability, 70*, 347–355. https://doi.org/10.1016/S0141-3910(00)00119-1

Nelson, M. L., & O'Connor, R. T. (1964). Relation of certain infrared bands to cellulose crystallinity and crystal lattice type. Part I. Spectra of lattices types I, II, III, and of amorphous cellulose. *Journal of Applied Polymer Science, 8*, 1311–1324. https://doi.org/10.1002/app.1964.070080322

Norkrans, B. (1950). Influence of cellulolytic enzymes from Hymenomycetes on cellulose preparations of different crystallinity. *Physiologia Plantarum, 3*, 75–87. https://doi.org/10.1111/j.1399-3054.1950.tb07494.x

Oh, S. Y., Yoo, D. I., Shin, Y., Kim, H. C., Kim, H. Y., Chung, Y. S., … Youk, J. H. (2005). Crystalline structure analysis of cellulose treated with sodium hydroxide and carbon dioxide by means of X-ray diffraction and FTIR spectroscopy. *Carbohydrate Research, 340*, 2376–2391. https://doi.org/10.1016/j.carres.2005.08.007

Pérez, J., Muñoz-Dorado, J., de la Rubia, T., & Martínez, J. (2002). Biodegradation and biological treatments of cellulose, hemicellulose and lignin: An overview. *International Microbiology, 5*, 53–63. https://doi.org/10.1007/s10123-002-0062-3

Saska, S., Barud, H. S., Gaspar, A. M. M., Marchetto, R., Ribeiro, S. J. L., & Messaddeq, Y. (2011). Bacterial cellulose-hydroxyapatite nanocomposites for bone regeneration. *International Journal of Biomaterials*. , Article 175362. https://doi.org/10.1155/2011/175362

Segal, L., Creely, J. J., Martin, A., & Conrad, C. M. (1959). An empirical method for estimating the degree of crystallinity of native cellulose using the X-ray diffractometer. *Textile Research Journal, 29*, 786–794. https://doi.org/10.1177/004051755902901003

Shi, X., Cui, Q., Zheng, Y., Peng, S., Wang, G., & Xie, Y. (2014). Effect of selective oxidation of bacterial cellulose on degradability in phosphate buffer solution and their affinity for epidermal cell attachment. *RSC Advanced, 4*, 60749–60756. https://doi.org/10.1039/C4RA10226F

Siondalski, P., Keita, L., Sićko, Z., Żelechowski, P., Jaworski, Ł., & Rogowski, J. (2003). Surgical treatment and adjunct hyperbaric therapy to improve healing of wound infection complications after sterno-mediastinitis. *Pneumonologia i Alergologia Polska, 71*, 12–16 (*in Polish*).

Siondalski, P., Keita, L. K., Żelechowski, P., Jagielak, D., & Rogowski, J. (2005). Clinical aspects of postoperative mediastitis in cardiac surgery. *Polish Journal of Thoracic and Cardiovascular Surgery, 2*, 38–43 (in Polish).

Siondalski, P., Roszak, K., Łaskawski, G., Jurowiecki, J., Jaworski, Ł., Brzeziński, M., Jagielak, D., & Rogowski, J. (2005). Chronic purulent sternum and ribs inflammation after a cardiac procedure successfully treated with omental plasty and hiperbaric oxygenation therapy after 44 months: Case report. *Case Reports and Clinical Practice Review, 6*, 216–219.

Siondalski, P., Siebert, J., Samet, A., Bronk, M., Krawczyk, B., & Kur, J. (2004). Usefulness of the PCR technique for bacterial DNA detection in blood of the patients after "opened heart" operations. *Polish Journal of Microbiology, 53*(3), 145–149.

Stanisławska, A., Staroszczyk, H., & Szkodo, M. (2020). The effect of dehydration/rehydration of bacterial nanocellulose on its tensile strength and physicochemical properties. *Carbohydrate Polymers, 236*, 116023. https://doi.org/10.1016/j.carbpol.2020.116023

Sugiyama, Perrson, J., & Chanzy, H. (1991). Combiner infrared and electron diffraction study of the polymorphism of native celluloses. *Macromolecules, 24*, 2461–2466. https://doi.org/10.1021/ma00009a050

Walseth, C. C. (1957). The influence of the fine structure of cellulose on the action of celluloses. *Tappi, 35*, 233–239.

Wang, B., Lv, X., Chen, S., Li, Z., Sun, A., Feng, C., Wang, H., & Xu, Y. (2016). *In vitro* biodegradability of bacterial cellulose by cellulose in simulated body fluid and compatibility *in vivo*. *Cellulose, 23*, 3187–3198. https://doi.org/10.1007/s10570-016-0993-z

Wang, J., Tavakoli, J., & Tang, T. (2019). Bacterial cellulose production, properties and applications with different culture methods – A review. *Carbohydrate Polymers, 219*, 63–76. https://doi.org/10.1016/j.carbpol.2019.05.008

Yakimets, I., Paes, S. S., Wellner, N., Smith, A. C., Wilson, R. H., & Mitchell, J. (2007). Effect of water on the structural reorganization and elastic properties of biopolymer films: A comparative study. *Biomacromolecules, 8*, 1710–1722. https://doi.org/10.1021/bm070050x